

NATIONAL RADIO ASTRONOMY OBSERVATORY  
GREEN BANK, WEST VIRGINIA

ENGINEERING DIVISION INTERNAL REPORT No. 107

140-FT POINTING ERRORS AFTER THERMAL SHIELDING

SEBASTIAN VON HOERNER

NOVEMBER 1977

NUMBER OF COPIES: 100

## Summary

The declination pointing error was monitored with electronic levels during 3/4 year on maintenance days. The thermal bendings of polar shaft and yoke, previously very large, are now negligible. The lower backup structure still gives errors of 23 arcsec max and 11 arcsec rms on a sunny noon, which is a factor of 5 down from noon values before shielding. Further improvement would require an expensive shielding of the backup structure.

Concrete building and polar shaft tilt by 30 arcsec between summer and winter, thus pointing parameters should be determined in spring or fall. An on-line thermal correction of two pointing parameters is suggested which leaves only 3.7 arcsec rms residuals for this tilt. The total rms DEC error will then be 5.7 arcsec at night, and 12.2 arcsec at 14:00 EST on sunny days, improved by a factor 3 by the shielding.

Second, we investigated pointing observations from K. Kellermann at  $\lambda = 2.8$  cm. The new least-squares program gave good agreement between the old 15 parameters and the new 11 ones (omitting redundancy and non-physical terms); but several strong error correlations call for a special sky distribution for future determinations. The observed DEC errors agree within 3.3 arcsec rms with those from simultaneous level monitorings. The observed rms errors at night are 6.1 arcsec RA and 5.0 arcsec DEC for stronger sources; they are 13.3 arcsec RA and 9.4 arcsec DEC for all sources in daytime.

Third, temperature differences in the upper structure were recorded continuously during 3/4 year. We suggest no on-line thermal corrections, but spraying the feed legs with foam. A thermal focal correction for shortest  $\lambda$  on sunny days may be discussed.

Fourth, the difference between prime focus and Cassegrain mode is investigated. Two (of the 11) pointing parameters will have different numerical values for both modes, but no additional parameters are required for the Cassegrain mode.

Fifth, the following pointing errors have been found negligible: from different weights of receiver boxes at prime focus; and from focal adjustments causing a rotational moment about the apex in Cassegrain mode.

I. Monitoring of Levels

Three electronic levels and four thermistors were monitored from Nov. 1976 to Sept. 1977, with four questions in mind:

How large is the remaining declination pointing error after shielding?

How much improvement has the shielding yielded?

What causes the remaining error?

Can the pointing be further improved?

1. Experimental Setup

Figure 1 shows the locations of the three levels, measuring NS inclinations:

$$\begin{array}{l}
A \text{ inside of sphere} \\
B \text{ at center of backup structure} \\
C \text{ at mount of tail bearing}
\end{array}
\left. \vphantom{\begin{array}{l} A \\ B \\ C \end{array}} \right\} (+ \text{ is South}). \quad (1)$$

Calling Dec = declination reading at console (+ is North), the pointing error then is

$$\epsilon = B + Dec \quad (+ \text{ is South}). \quad (2)$$

And the part of the pointing error occurring above the sphere (from thermal deformations of yoke, declination wheel, and backup structure) we call

$$Y = B + Dec - A. \quad (3)$$

Temperatures were measured with four thermistors shown in Fig. 1, mounted at the outside of shaft and yoke arms under the shielding foam. We shall use:

$$\begin{aligned}
\Delta T_s &= T_1 - T_2 = \text{temperature difference across polar shaft,} \\
\Delta T_y &= T_3 - T_4 = \text{temp. difference across west yoke arm,} \\
T_y &= \frac{1}{2}(T_3 + T_4) = \text{average yoke temperature} = \text{air temperature smoothed over a time constant of about three days.}
\end{aligned} \quad (4)$$

Notes were also taken about the degree of cloudiness and about precipitation. But as a quantitative measure of sunshine versus cloudiness we use, as in previous reports,

$$\Delta T_{\text{air}} = \text{raise of ambient air temperature, from 8:00 EST to its maximum at about 15:00 EST} = \text{measure of sunshine.} \quad (5)$$

Readings (of levels, thermistors, ambient air, wind, and Dec) were taken:

1. once per hour during all maintenance periods;
2. occasionally in between observations, at about 7-8 EST and 13-14 EST.

The shielding foam on tower, shaft and yoke arms, and the electric heat pads and foam on parts of the platform, had been installed on Sept. 3-7, 1976, before the present monitoring period. During this period, three changes occurred.

1. On January 19, 1977, the electric heat pads were turned on, regulated to about 18 °C. This turned level C by +7 arcsec (south), and levels A and B by -6 arcsec (north). All previous readings then were corrected by these amounts.

2. During the first days of May, 1977, level B was remounted a bit sideways, for reducing any interference with work at the vertex. This changed level B by -48 arcsec (north), and 48 arcsec were added to all following readings of B.

3. On June 8, 1977, two fans were mounted inside the polar shaft, circulating the air about the polar axis, for reducing the temperature difference  $\Delta T_s$ .

An inspection of the data seemed to show that the zero of level B might have changed by about +11 arcsec on Dec. 28, by +19 arcsec on March 17, and by -22 arcsec on Aug. 1, maybe caused by work at the vertex. These changes were not corrected for, but different symbols are used in Figs. 2 - 5:

+	Nov. 10 - Dec. 27	}	zero change of B	
x	Dec. 28 - March 16	}	zero change of B	
●	March 17 - June 7	}	fans mounted in shaft	(6)
o	June 8 - Aug. 1	}	zero change of B	
Δ	Aug. 2 - Sept. 14	}	zero change of B	

Because of this uncertainty regarding the zero of level B, and because observing periods mostly last only a few days and being with a calibration of the box-offset (which eliminates the need for an absolute zero), the following analysis will mostly use the difference  $D^n$  between readings taken n days apart.

## 2. Concrete Building and Polar Shaft

Fig. 2 shows the tilt of the tail bearing, C, as a function of the smoothed air temperature,  $T_y$ . For 75 readings, all at 8:00 EST, we find

$$\begin{aligned}
 \text{Level C:} \quad A_v &= +6.49 \text{ arcsec} \\
 \text{ptp} &= 8.20 \text{ arcsec} \\
 \text{rms}(C-A_v) &= 2.05 \text{ arcsec}
 \end{aligned}
 \tag{7}$$

There is practically no correlation left after the shielding:

$$|C/T_y| \leq 0.10 \text{ arcsec}/^\circ\text{C}.
 \tag{8}$$

Before the shielding (see Fig. 10 of Engin. Rep. No. 100, May 1976), level C had a peak-to-peak range of 42 arcsec, and a correlation of 1.06 arcsec/ $^\circ\text{C}$ . The improvement thus is a factor of 5.1 for the ptp, and at least 10 for the correlation.

Readings of level A inside the sphere, again at 8:00 EST, are shown in Fig. 3a as a function of the temperature  $T_y$ . We see a well-pronounced negative correlation,

$$A/T_y = (-0.76 \pm 0.08) \text{ arcsec}/^\circ\text{C}.
 \tag{9}$$

This correlation is confirmed in Fig. 3b by plotting the changes occurring after 7 days,  $D^7A$  versus  $D^7T_y$ , which removes any possible zero shifts. We call

$$A_o = A + 0.76 T_y \quad (10)$$

the residuals after removing the correlation. They are shown in Fig. 3c as a function of the temperature difference  $\Delta T_s$  across the polar shaft, checking for internal shaft bending; there might be some correlation, but the scatter is larger than that, and the ptp range of  $\Delta T_s$  is only 1.6 °C after shielding, which is an improvement of a factor 7. We find for 64 readings, in arcsec,

	level A	residual $A_o$
Av	-4.67	-4.77
ptp	29	20
rms(A - Av)	8.06	3.71

(11)

In summary, we find a very good improvement for building and shaft. The shaft bending is now small enough to be neglected; and the tilt of the whole building and polar axis, as expressed by (10), could be removed by the pointing program in the on-line computer, leaving an rms residual of only 3.7 arcsec. The latter is even much smaller after installing the two fans in the shaft, see Fig. 3,c.

### 3. Deformations Above the Sphere

We call Y the part of the pointing error occurring above the sphere, as defined in (3). Fig. 4a shows Y as a function of the temperature  $T_y$ , for readings at 8:00 EST. On first glance, there is a weak positive correlation. But a closer inspection leads to the suspicion that the zero of level B might have changed three times as explained with (6). The suspicion is confirmed

in Fig. 4b by plotting the 7-day differences, showing indeed no correlation, and the same negative result is obtained by the 14-day differences of Fig. 4c. We thus conclude that Y is not influenced by the temperature itself (it would be very amazing if it were).

In Fig. 4d we check for internal bending of the yoke arms, which was by far the largest error contribution before shielding. Since there is no obvious correlation between the 14-day changes of Y and those of  $\Delta T_y$ , we conclude that the scatter of Y in Figs. 4b and 4c is not caused by the yoke arms anymore, but probably by the backup structure. Any further improvement then would need either a foam-spray on the whole backup structure, or an enclosure of the backup structure similar to the one at the 7-m Bell telescope; both are quite expensive.

#### 4. The Declination Pointing Error at 8:00 EST

Fig. 5a shows the pointing error as defined in (2), as a function of the temperature  $T_y$ . It shows again a large scatter but not much correlation, similar to Fig. 4a, again explained by zero shifts of level B. The 7-day changes of Fig. 5b yield indeed a negative correlation of about the same slope as Figs. 3a and 3b for level A, as to be expected, which could be corrected in the computer.

For any observing program where pointing matters, the observer should first calibrate his box offset by observing some strong point sources of known position. What matters then is the change of  $\epsilon$  from thereon until the end of his program. Fig. 6 shows the changes of A, Y and  $\epsilon$  after 1, 3, 7 and 14 days. We see a strong systematic increase of A with time, as expected from correlation (9), whereas Y stays much more constant, indicating deformations which are less correlated from one day to the next. The resulting error  $\epsilon$  shows some increase

with time, which means the observer is advised to recalibrate during longer programs, say every third day, and preferably at night.

Evaluating our old data before shielding in the same way, we find for the 8:00 EST readings in the average an improvement for the pointing error of a factor three:

	before shielding	now		
$D^1_\epsilon$	17.9	5.3	}	rms, arcsec. (12)
$D^3_\epsilon$	24.0	7.1		
$D^7_\epsilon$	17.6	8.7		

5. Dependence on Hour Angle

Fig. 3a and correlation (9) show a fairly large tilt of the sphere between summer and winter, which we interpret as a tilt of the polar axis because the internal shaft bending is only small according to Fig. 3 and according to the small rms residuals of (11). A calibration of the box offset will correct for this axial tilt only at the meridian and close to it, but not for larger hour angles. This is different for the deformations Y of the upper structure which act just the same as a box offset and thus are omitted by its calibration, for all hour angles.

In Table 4 of Engin. Report 102 (Nov. 1976) the NS box offset gives a constant ( $I_1$ ) for all pointings, whereas a NS tilt of the polar axis ( $I_6$ ) gives a declination error proportional to  $\cos H$ , where  $H$  = hour angle. Thus, if an axial tilt is corrected for by a box offset calibration, the residual pointing error is proportional to  $1 - \cos H$ .

The ptp range of temperature  $T_y$  is 40 °C, and with correlation (9) this gives a ptp range for the axial tilt of  $0.76 \times 40 = 30.4$  arcsec. We mentioned already that this tilt can be corrected for in the on-line computer, using the



value  $T_y$  as measured during the observation. However, if this correction is not applied, then the pointing parameters should be determined by observations done in spring or fall, and the declination error after box calibration will be half the full range:

$$\epsilon(H) = 15.2 (1 - \cos H) \text{ arcsec, in summer and winter;} \quad (13)$$

or, in the average over the whole year, with  $15.2 / \sqrt{2} = 10.7$ ,

$$\epsilon(H) = 10.7 (1 - \cos H) \text{ arcsec, rms of whole year.} \quad (14)$$

If we take a further average over the range of hour angle mostly used, we find

$$\epsilon_H = 4.2 \text{ arcsec, rms for } -5^h \leq H \leq +5^h, \text{ whole year.} \quad (15)$$

This rms error of 4.2 arcsec looks rather small and might be considered negligible. But keeping in mind the maximum error of 15.2 arcsec during several months in summer and winter at  $H = \pm 6^h$ , we still think the on-line correction is advisable.

### 5. Changes during Sunny Days

Fig. 7 shows the thermal deformations of A, Y and  $\epsilon$  during some sunny days. These deformations were measured between 8 and 16 EST for a total of 43 days. We call  $D^0$  the largest deviation from the 8:00-value, and find

x =	$D^0A$	$D^0Y$	$D^0\epsilon$	
$n(x > 0)$	4	18	15	} numbers
$n(x < 0)$	34	24	28	
$\max(x)$	+4	+14	+14	} arcsec
$\min(x)$	-11	-18	-23	
rms(x)	3.44	8.07	10.04	

(16)

The deformations of A are only small and almost all are negative (north). They are neither correlated with  $D^{\circ}\Delta T_s$  nor with  $D^{\circ}T_y$ , but are correlated with  $\Delta T_{air}$ ; they are probably caused by an elongation of the platform under sunshine, and shall not be further investigated.

Most striking is the symmetry of  $D^{\circ}Y$  regarding sign. Before shielding, all  $D^{\circ}Y$  were negative in sunshine (N), and of much larger amounts (70 arcsec max). In Fig. 8a we see that the scatter of  $D^{\circ}Y$  increases with  $\Delta T_{air}$  which means the daily deformations are caused by sunshine. And Fig. 8b shows that  $D^{\circ}Y$  and its sign depend on the Sun's declination (especially if the telescope has not been moved in between). This means that  $D^{\circ}Y$  is caused by sunshine on the various parts of the backup structure, the result depending on which parts are warmed up and when. Unfortunately, an improvement could only be achieved by a thermal shielding of the whole backup structure.

The pointing errors as shown in Fig. 7c can be compared with similar data before shielding (Electronics Div. Report 164, Dec. 1975). Selecting in both cases all sunny days with  $\Delta T_{air} \geq 10^{\circ}C$ , we find for the sun-induced maximum pointing error  $D^{\circ}\epsilon$  an improvement of a factor of five:

	before shielding	now	
$\max  D^{\circ}\epsilon $	105.0	23.0	} arcsec
$\text{rms}(D^{\circ}\epsilon)$	60.3	10.8	

(17)

Although these sun-induced errors can be occasionally quite large, 23 arcsec, and amount to 10 arcsec for the rms of all days, they are of short duration. Spread out over the 24 hours of a day, we find

$$\text{rms}(D^{\circ}\epsilon) = 4.9 \text{ arcsec, } \text{rms all days 24 hours.} \quad (18)$$

6. The Total Pointing Error

We consider a 3-day observing period, or a recalibration of the box off-set every 3 days for longer periods. The 8:00 EST error is 7.1 arcsec after 3 days according to (12), and we find 5.7 arcsec for its rms during the 3 days. This then is the rms declination pointing error, during nights or cloudy days, and close to the meridian.

At 14:00 EST we must add quadratically 10.8 arcsec for sunny days according to (17), but only 4.9 arcsec if the rms is taken over all 24 hours and any weather according to (18). For observations at an hour angle of  $H = \pm 6^h$ , we add quadratically 10.7 arcsec in the average over the whole year according to (14), if the pointing parameters have been determined in spring or fall. This yields the following rms pointing errors:

	close to meridian	at $H = \pm 6^h$	
night or clouds	5.7	12.1	} arcsec (19)
at 14:00 EST, if sunny	12.2	16.2	
rms of 24 hours, all weather	7.5	13.1	

7. Possible Improvements

If the pointing parameters are always corrected for the present temperature, then the errors at any hour angle will be just as small as they are close to the meridian, thus making the last column of (19) obsolete. For this purpose, we must feed the two thermistor outputs from the West yoke arm into the computer and get the average,  $T_y = \frac{1}{2}(T_3 + T_4)$ . We use the pointing parameters in the notation of equations (15) and (16) of the Engineering Division Internal Report No. 102 (Nov. 1976), with the sign convention

$$\Delta D = (\text{observed console declination}) - (\text{source catalog declination}) \quad (20)$$

and similar for the hour angle. We call  $P_{3,0}$  and  $P_{10,0}$  the values of parameters  $P_3$  and  $P_{10}$  as obtained by their last determination, preferably in spring or fall, at a yoke temperature of  $T_0$ . The pointing program in the computer then must use for the present values

$$\begin{aligned} P_3 &= P_{3,0} - 0.76 (T_y - T_0), \\ P_{10} &= P_{10,0} - 0.76 (T_y - T_0). \end{aligned} \quad \left. \begin{array}{l} T \text{ in } ^\circ\text{C} \\ P \text{ in arcsec} \end{array} \right\} \quad (21)$$

Any further improvement, however, would need a thermal shielding for the whole backup structure, which would be costly and awkward.

## II. Astronomical Pointing Observations

### 1. Observational Data

The observations were done by K. Kellermann, from Dec. 2, 14:50 EST, to Dec. 4, 14:05 EST, in 1976; at  $\lambda = 2.82$  cm wavelength ( $\nu = 10.65$  GHz), with 120 °K system noise, and at the prime focus. The weather was sunny and clear, with  $\Delta T_{\text{air}} = 15$  °C.

The on-line refraction correction used the detailed weather information from the interferometer, and the improved correction for the curvature of the Earth, see equations (14) and (15) of Engin. Report No. 101, May 1976. The thermal shielding was all installed, but the heat pads were not yet turned on.

For the data evaluation, a computer program by Tom Cram and Claude Williams applied two fits to each scan: first, a rough fit of a Gaussian using all data of the scan, obtaining the height and width of the Gaussian; second, a fine fit of a Gaussian of this height and width, using only the upper third of the data, and obtaining the source position (in right ascension or declination).

The sources observed were the 18 calibration sources of the 1973 Report of Gordon, Huang, Cate, Kellermann and Vance. A total of 151 scans was observed, each one in both right ascension and declination. From these we omitted three bad scans (of low flux) with errors between 1.5 and 4.2 arcmin. The remaining 148 scans were divided into night and day observations:

$$\begin{aligned} & 2 \text{ nights, } 20:00 - 7:00 \text{ EST, } 68 \text{ scans;} \\ & 3 \text{ days, } 7:00 - 20:00 \text{ EST, } 80 \text{ scans.} \end{aligned} \tag{22}$$

The distribution of the 68 night scans over the available sky is shown in Fig. 9. We see a fairly even coverage. Unfortunately, there are only two weak sources far north, and also the two southern sources are only weak ones.

## 2. Old and New Pointing Parameters

The old 15 pointing parameters were discussed in Engin. Report No. 102 of Nov. 1976. A new set of 11 parameters was suggested, omitting redundancy and non-physical parameters. A least-squares method was presented, yielding not only the 11 parameters but also their mean errors and their correlation matrix. The programming of this method, and its application to the observational data, were done by Claude Williams.

Table 1 gives a comparison of both sets of parameters, their physical causes, and their angular terms in the pointing equation; with  $c = \cos$ ,  $s = \sin$ ,  $D = \text{declination}$ ,  $H = \text{hour angle}$ ,  $Z = \text{zenith distance}$ ,  $L = 38.4^\circ$ , and  $Q = K / \{cZ + 0.00175 \tan(Z - 2.5^\circ)\}$ , where  $K$  is the weather-dependent refraction term of Engin. Report No. 101, May 1976. Furthermore, NP = not perpendicular, Polax = polar axis, Decax = declination axis, Mt = mounting (shaft and yoke), and Grav = gravitational deformations.

Table 1 gives also the numerical values of the parameters, determined from observations in 1973, 1975 and 1976. The present 1976 pointing data of the 68 night scans were solved for both sets of (15 and 11) parameters. A comparison of these numerical values shows a positive result: for all those parameters where the 15-parameter solutions of 1975 and 1976 agree with each other ( $P_2, P_3, P_5, P_7$ ), the 15-parameter and the 11-parameter solutions also agree within the mean error of the latter. This may be counted as a confirmation for our new least-squares solution.

## 3. Error Correlation

A second result of Table 1 is the following: for all parameters where the 15-parameter and the 11-parameter solutions disagree ( $P_9, P_{10}, P_{11}$ ), we have also a strong disagreement between the 15-parameter solutions of 1975 and 1976. This can be explained by the strong correlation between these three parameters.

Table 1. The new 11 pointing parameters; compared with the old 15 parameters after removing their redundancy (in arcmin) with  $\Delta h = \cos D \Delta H$ .

New 11 Param.	Physical cause	Angular terms		Old 15 Param.	Prime Focus			Cassegrain 15 Param. Kellermann 1975
		$\Delta D$	$\Delta h$		Gordon 1973	Old 15 Param. Kellermann 1975	Present 1976	
P <sub>1</sub>	Box N, Dial D	1		A <sub>2</sub>		1.71		1.64 ± .05
P <sub>2</sub>	Polax E	sH	-SDcH	A <sub>8</sub>	-.53	-.55	-.52	-.55
P <sub>3</sub>	Polax N, Grav Mt	cH		A <sub>7</sub> + A <sub>14</sub>	-1.55	-2.08	-2.11	-2.05
P <sub>4</sub>	Grav Dish N	sDcH - tLcD		cLA <sub>5</sub> + A <sub>12</sub>	.63	.68	.94	.67
P <sub>5</sub>	Refraction	Q(sL-sDcZ)/cD	-QcLsH	A <sub>3</sub>	1.08	.97	1.04	.98
P <sub>6</sub>	Box E, Beam NP Decax		1	-A <sub>6</sub>		-.63		-.57
P <sub>7</sub>	Decax NP Polax		sD	-A <sub>9</sub>	-1.32	-1.24	-1.12	-1.23
P <sub>8</sub>	Dial H		cD	-A <sub>1</sub>		1.04	1.55	.95
P <sub>9</sub>	Grav Dish E		sH	A <sub>4</sub>	2.32	-.11	1.54	1.45
P <sub>10</sub>	Polax N, Grav Mt		sD <sub>sH</sub>	A <sub>7</sub>	-1.98	.14	-1.18	-1.50
P <sub>11</sub>	Grav Mt		cD <sub>sH</sub>	A <sub>11</sub>	-2.00	-.09	-1.52	-1.74
	no phys. cause		sDcD <sub>sH</sub>	A <sub>10</sub>	1.53	-1.72	.60	
			sD		A <sub>13</sub>	.24	-.06	-.19

Table 2. Mean errors  $\epsilon_i$ , and normalized correlation coefficients  $c_{ij}$ , of the new 11 pointing parameters.

$P_i$	$\Delta D$	$\Delta h$	$\epsilon_i$	$c_{ij}$															
				$P_1$	$P_2$	$P_3$	$P_4$	$P_5$	$P_6$	$P_7$	$P_8$	$P_9$	$P_{10}$						
$P_1$	1		.05	1															
$P_2$	sH	sDcH	.03	-.37	1														
$P_3$	cH		.06	-.61	.28	1													
$P_4$	sDcH-tLcD		.07	.57	-.20	-.12	1												
$P_5$	Q(sL-sDcZ)/cD	QcLsH	.02	.23	-.11	-.21	.73	1											
$P_6$		1	.11	.02	-.08	-.01	-.02	-.04	1										
$P_7$		sD	.06	-.13	.33	.10	-.09	-.07	-.58	1									
$P_8$		cD	.13	-.01	.05	.00	.04	.06	-.97	.50	1								
$P_9$		sH	.21	.10	-.11	-.08	.24	.31	-.48	.07	.51	1							
$P_{10}$		sDsH	.13	-.06	.05	.06	-.18	-.25	.25	-.11	-.29	-.85	1						
$P_{11}$		cDsH	.19	-.05	.09	.04	-.08	-.10	.52	-.10	-.54	-.95	.74						



Table 2 gives the matrix of the correlation coefficients  $c_{ij}$  (normalized to  $-1 = c_{ij} = +1$ ). As explained in Eng. Report 102,  $c_{ij}$  is the correlation between the error of parameter  $P_i$  and the error of  $P_j$ . We see that the error of  $P_9$  shows a strong negative correlation with the errors of  $P_{10}$  and  $P_{11}$ . This means that the values of the three parameters are very uncertain, but that the sums  $P_9 + P_{10}$  and  $P_9 + P_{11}$  should have well-defined values. This is checked and confirmed in Table 3: for both sums, all four determinations agree with each other within the mean error (the quadratic sum of the two errors from Table 1).

Table 3. Combinations of correlated parameters.

	15-parameter solutions			11-par.	average	mean error
	1973	1975	1976	1976		
$P_9 + P_{10}$	+0.34	+0.36	+0.03	-0.05	+0.17	0.25
$P_9 + P_{11}$	+0.32	+0.02	+0.02	-0.29	+0.02	0.28

In addition to the correlations discussed above, we have in Table 2 another strong correlation between  $P_6$  and  $P_8$ . Comparing the angular terms of these two parameters, we find that the least-squares solution has difficulties to see the difference between  $l$  and  $cD$ , which means that we did not have enough observations at high declinations close to the pole, which is easily confirmed by looking at Fig. 9. As to the correlation between  $P_9$ ,  $P_{10}$  and  $P_{11}$ , the solution has difficulties seeing the differences between  $sH$ ,  $sDsH$  and  $cDsH$ , which means that we should have, at extreme hour angles, more observations at extreme declinations. This again is obvious from Fig. 9, but hard to change.

For future pointing programs, one should not try to cover the full range of sky evenly; but instead one should concentrate some observations close to the center at  $D = 0$  and  $H = 0$ , and have many observations just as close as possible

to the horizon and to the telescope limits. And observations at highest and lowest declinations should be repeated many times, because of the weakness of these sources.

4. Pointing Errors

The rms pointing errors as derived from various astronomical observations are given in Table 4. The first line shows how large the errors would be if we did not apply any on-line pointing corrections: about 2 arcmin in hour angle, and 1.5 arcmin in declination. Lines 2, 3 and 4 were observed before the thermal shielding was installed. While the older determinations of the 15 pointing parameters used all available data (second line), it was later realized that the parameters should be determined from night observations only, avoiding the large non-repeating thermal deformations from sunshine (third line); this gave a good reduction of the residual errors. The day observations were then evaluated by using the parameters which were obtained from the night observations, line 4.

Table 4. RMS pointing errors of 140-ft ( $\Delta h = \cos D \Delta H$ )

Observations	night day	n	parameters	$\Delta h$	$\Delta D$	Notes:
1. Present, 1976	all	148	all $A_1 \cdots A_{15} = 0$	115	89	No pointing corrections
2. Gordon, et al, 1973	all		own 15	31	25	before thermal shielding
3. Kellermann, 1975	night		own 15 = standard	12	12	
4.	day		standard 15	13	25	
5. Present, 1976	night	68	own 15	7.0	6.2	after thermal shielding
6.	day	80	15 from night	11.6	9.7	
7. Present, 1976	night	68	own 11	8.3	6.2	
8.	day	80	11 from night	13.3	9.4	
9. Present, strong sources	night	42	11 from all 68, night	6.1	5.0	
10. From monitoring levels, predicted			{	night	5.7	
11.				day	8.9	

The present observations after thermal shielding are shown in lines 5 and 6 of Table 4, solved for the old set of 15 parameters. The errors are reduced by at least a factor 2 by the shielding. The 11-parameter solution (lines 7 and 8) gives similar results. If we omit the five faintest sources, which have higher intrinsic errors because of their low signal/noise ratios, then the remaining 42 night scans (using the 11 parameters obtained from all 68 night scans) yield for the rms pointing errors of the telescope the nice and low values of line 9:

$$\left. \begin{array}{l} \Delta h = 6.1 \text{ arcsec} \\ \Delta D = 5.0 \text{ arcsec} \end{array} \right\} \text{rms, strong sources at night.} \quad (23)$$

Fig. 10 shows both pointing errors as a function of the time of the day, for all three days and two nights of the observing period. The influence of the sunshine is still clearly seen, although greatly reduced by the shielding.

#### 5. Comparison with Electronic Levels

We would like to compare the astronomically observed pointing errors with the errors to be expected from the monitoring of the electronic levels of Section I. Line 10 in Table 4 is taken from (19) without the hour angle effect of Section I,5, because in the present observations there is no seasonal time lag between the determination of the parameters and their use; line 11 then is the rms over the 13 hours of the day according to (22). We find indeed a very good agreement between the expected errors of lines 10 and 11, and the observed ones of lines 7, 8 and 9.

In order to allow a more detailed (simultaneous) comparison, the pointing observations of Dec. 2 - 4 had been interrupted 23 times, the telescope then was pointed at zenith (console dials), and a reading of level B was taken. The deviation of level B from its night average is shown in Fig. 11 for all

cases where astronomical pointing errors were measured within 30 minutes before or after the reading of level B. We see a very good correlation between the two; which means that the location of level B, above the center of the declination axis in the middle of the heavy backup structure, is indeed representative for the telescope's pointing direction. The deformations of the upper structure and feed legs then can only give minor contributions to the pointing errors, with an occasional maximum of 6 arcsec.

While the 33 observed pointing errors of Fig. 11 give an rms of 7.4 arcsec, their deviation from the straight line of slope 1.0 (difference between observation and level reading) gives only an rms of 3.3 arcsec. We may regard these 3.3 arcsec as a measure or upper limit of the intrinsic pointing accuracy given by system noise, encoder readings, and electronic loops for reading and pointing.

#### 6. Comparison with B. Turner's Results

Barry Turner (Memo Oct. 28, 1977) observed at the Cassegrain focus with the new maser at  $\lambda = 1.35$  cm. He finds an (unexplained) beam splitting into three beams at low elevations. He finds also larger pointing errors when peaking up on the main beam, with a peak-to-peak range of 60 and an rms of 12 arcsec in right ascension, and somewhat larger in declination.

These pointing errors can be explained by the beam splitting. The distances between beams of comparable height in his Figs. 9 and 10 show a range from 1.8 to 2.7 and an average of  $2.1$  arcmin, whereas the standard parameters of the on-line pointing program were determined at  $\lambda = 2.8$  cm where the (unsplit) beam peaks close to the center of gravity. Thus, deviations of up to 1 arcmin are to be expected.

Furthermore, if the determination of the parameters and their use are done at different temperatures, some pointing errors will result from the hour angle

effect of Section I,5, see also equations (21). Finally, pointing parameters for Cassegrain and prime focus are somewhat different, see Section IV.

Beamsplitting or stronger unsymmetric sidelobes (see Engin. Report No. 103, Febr. 1977) would represent a major problem for short wavelengths, not only because of the loss of gain and resolution, but also because the pointing then would depend on wavelength. Future observations (including optimum focussing) and investigations of these beam shape effects are now in preparation. Furthermore, the deformable subreflector was originally planned to correct only the gravitational astigmatism (IEEE Transact. Ant. + Propag. March 1978) which is a one-parameter deformation, but the subreflector actually has four actuators giving us four degrees of freedom for its use. We hope we will be able to correct also these beam effects, at least to some degree. If these effects are confirmed by new observations, and if the deformable subreflector cannot correct them well enough, we should reconsider our pointing definition: either continue with the present method of peaking up on the highest lobe (maximum gain, but pointing parameters depending on wavelength and getting ambiguous in case of comparable lobe heights); or defining the pointing by the center of gravity of the whole beam (less gain, but no wavelength-dependence nor ambiguity).

### III. Temperature Measurements in the Upper Structure

#### 1. Experimental Setup

We want to know how much the pointing of the 140-ft might be affected by temperature differences  $\Delta T$  in the upper structure. For this purpose, 10 thermistors were mounted on structural members: 4 thermistors at the feed support legs at medium height (one at each leg); one at the center of the declination shaft, and one at the nadir point of the declination wheel (these two concern the change of focal length and not the pointing); and four thermistors in the cantilevering outer part of the dish support structure. The ambient air temperature was measured, too.

Recordings were taken continuously with a 12-pen graphical recorder during 270 days and nights from Dec. 1, 1976 to Sept. 1, 1977. After a visual inspection of all recordings, we selected for a numerical reading of the data the following four periods:

1. Dec. 2, 12:00 - Dec. 4, 15:00    pointing observations
2. April 12, 0:00 - 24:00            largest  $\Delta T$
3. Dec. 11, 0:00 - 24:00            smallest  $\Delta T$
4. March 20, 0:00 - 24:00          average  $\Delta T$

Mounting of the thermistors, their recording, and reading the data were all done by Fred Crews.

#### 2. Numerical Data

The main results are summarized in Table 5. The largest temperature differences measured, between couples of corresponding members, amount to 3 - 4 °C. The larger differences occur on sunny days along the z-axis between declination shaft and wheel (focal length), and opposite feed legs (pointing).

But the cantilevering rim support (pointing) shows only smaller differences, with 1.5 °C maximum. The 24-hour rms values of  $\Delta T$  for an average medium sunny day are all below 0.7 °C.

Table 5. Measured temperature differences,  $\Delta T$ , in the upper structure (in °C).

day (notes)	duration hours	ambient air temper.	temperature differences $\Delta T$		
			feed legs SE-NW	declin. wheel -shaft	cantilever NE top- bottom
Dec. 2-4, 1976 (pointing obs.)	51	max +5.5 min -17.2	max +1.4 min - .7 rms .46	+3.8 -1.3 1.41	+1.5 - .9 .41
April 12 1977 (largest $\Delta T$ )	24	max +23.2 min + .6	max +1.3 min -3.1 rms 1.40	+3.3 -1.2 1.83	+1.1 - .7 .38
Dec. 11 1976 (smallest $\Delta T$ )	24	max +7.8 min +4.6	max + .3 min - .2 rms .12	0.0 - .9 .54	+ .3 - .3 .15
March 20 1977 (average $\Delta T$ )	24	max +11.1 min + .6	max 0.0 min -1.0 rms .61	+1.3 0.0 .65	+ .1 - .7 .39

Fig. 12,a shows the measured temperatures as a function of time, for the most extreme day. We see a considerable time lag of several hours for the heavy shaft as compared to ambient air, and the feed legs can get up to 5.5 °C warmer than the air due to sunshine. Fig. 12,b shows the differences  $\Delta T$ . During the night they are all small,  $|\Delta T| \leq 1.1$  °C, from 19:00 to 7:00 EST. Large differences between opposing feed legs occur between 11:00 and 17:00. Fig. 13 gives the same kind of data for an average day.

### 3. Resulting Pointing Errors

The pointing errors  $\Delta\phi$  to be expected from structural thermal differences  $\Delta T$  have been estimated, with a crude model, in Electronics Div. Int. Report 164 (Dec. 1975). We found, for the feed legs,

$$\Delta\phi = 5.84 \text{ arcsec } \Delta T / ^\circ\text{C} \quad (24)$$

where the beam goes south if the southern legs get warmer. And for the cantelever, we found

$$\Delta\phi = 5.34 \text{ arcsec } \Delta T / ^\circ\text{C} \quad (25)$$

where the beam goes north if the upper part of the northern cantelever gets warmer. If we tolerate pointing errors up to 5 arcsec, say, then temperature differences for feed legs and cantelever are tolerable up to 1 °C. This then means, from our numerical data, that all errors at night are tolerable, and so are the 24-hour rms errors except for the most sunny days. But the maximum pointing errors shortly after noon, on extremely sunny days, would be too large, and one might consider installing an on-line thermal pointing correction which uses the temperature measurements from the feed legs.

But equations (24) and 25) resulted only from crude estimates. We must first check whether they are valid (correlated data) and useful (well above the scatter), and if so, their numerical values must be calibrated empirically. If they are valid and useful, we should see a good negative correlation between the measured  $\Delta T$  (feed legs) and the observed residual pointing errors from Fig. 11 (deviation from straight line of slope 1.0). And we should see a positive correlation between  $\Delta T$  (cantelever) and these residuals.

The expected correlations are checked in Fig. 14. The result is negative: if there are such correlations, they are blurred by the scatter of the data. Which means we should not install a thermal pointing correction. Actually,



this result was already indicated at the end of Section II,5 by the small amount of rms(residual) = 3.3 arcsec. We do suggest, however, to spray the feed legs with foam, which may help and cannot hurt.

#### 4. Resulting Focal Change

The change of focal length to be expected from a thermal gradient along the z-axis has been estimated, again with a crude model, in Electronics Div. Int. Report 160 (May 1975). Applied to our present thermistor locations (declination shaft and wheel), we expect

$$\Delta F = 1.3 \text{ mm } \Delta T / ^\circ\text{C}. \quad (26)$$

The gain loss from axial defocussing was given in the same Report as

$$L = \frac{G_o - G}{G_o} = \frac{1}{16} (\pi \Delta F / \lambda)^2 = 0.548 (\Delta F / \lambda)^2. \quad (27)$$

If we tolerate a loss of 3%, say, then we must have

$$\Delta F \leq 0.234 \lambda \quad (28)$$

and with (26)

$$\Delta T(\text{dec shaft - wheel}) \leq 1.80 \text{ } ^\circ\text{C } \lambda / \text{cm}. \quad (29)$$

We see from Table 5 that this condition is fulfilled for  $\lambda \geq 1.0$  cm for all the 24-hour rms values of  $\Delta T$ , but not for the maximum  $\Delta T$  at noon on extremely sunny days. The largest value measured is  $\Delta T = 3.8$   $^\circ\text{C}$ , and a gain loss  $\geq 3\%$  would then result for wavelengths  $\lambda \leq 2.1$  cm, for example

$$L = 7.9\% \text{ for } \lambda = 1.3 \text{ cm, at sunny noon.} \quad (30)$$

Since defocussing was not measured with the present observations (Dec. 2 - 4), we cannot check these expectations at present. Furthermore, whether the gain loss

as estimated above is large enough to warrant a thermal on-line focus correction, is somewhat doubtful and should be decided by the observers. If so, we would first need an empirical check and calibration for equation (26). Any thermal defocussing would also be somewhat improved if the feed legs were sprayed with foam.

#### IV. Cassegrain and Prime Focus Parameters

##### 1. General

The gravitational deformations of dish and feed legs are drawn in Fig. 15. A detailed inspection shows that going from prime mode to Cassegrain mode cannot introduce any new pointing parameters, but it will change the numerical values of the two parameters  $P_4$  (gravity dish North) and  $P_9$  (gravity dish East), see Table 1. This change has three causes. First, the Cassegrain mirror is heavier than the prime focus receiver box, yielding a larger lateral movement  $A$  of the leg apex. Second, this movement  $A$ , and the movement  $W$  of the best-fit focus, enter the pointing offset  $\phi$  for both modes with different factors. Third, two items matter for Cassegrain mode only: the angular rotation  $\beta$  of the feed apex (holding the Cassegrain mirror), and the lateral movement  $T$  of the Cassegrain feed tower.

All deformations shown in Fig. 15 have been computer-calculated with structural analysis by W. Y. Wong. In principle, the analysis should agree with  $P_4$  and  $P_9$  from astronomical observations. But the 140-ft is a rather awkward and complicated structure, difficult to replace by a model. The calculated deformations  $T$  and  $A$  should be reliable. But most unreliable is the vertex shift  $V$  of the best-fit paraboloid for the deformed dish, because it depends on the local curvature of the surface, which is only the second derivative of the deformations. The resulting uncertainty of  $V$  then also

causes uncertainties of the rotation  $\alpha$  of the axis, and of the shift  $W$  of the best-fit focus. Another uncertain quantity is the apex rotation  $\beta$ , because it depends on the shear stiffness of the round and complicated donut structure. Unfortunately,  $V$  and  $\beta$  are the largest deformations; thus, computed and observed pointing deviations  $\phi$  do not agree. Nevertheless, we will give the details in order to show how the difference between the two modes is defined structurally, and for some additional estimates.

## 2. Definitions and Analysis

We define the following deformations and their signs:

$V$  = vertex shift of best-fit paraboloid, down

$\alpha$  = rotation of paraboloid axis, up

$A = A_o + A_w$

$A_o$  = shift of leg apex (dead weight + sterling), down

$A_w$  = shift of leg apex (weight of prime box,  $w = p$ , or of Cassegrain,  $w = c$ )

$\beta$  = apex rotation for Cassegrain, up

$T$  = shift of Cassegrain feed tower, down

The loads at the apex are:

$S = 1240 \text{ lb} = \text{sterling mount}$

$P = 850 \text{ lb} = \text{prime focus receiver box}$

$C = 2050 \text{ lb} = \text{Cassegrain mirror, mounting + counterweight}$

The structural analysis yields, for movement from zenith along meridian to horizon:

$V = 1.76 \text{ inch}$

$\alpha = 1.65 \times 10^{-3} \text{ rad} = 5.67 \text{ arcmin}$

$A_o = 0.271 \text{ inch}$

$A_p = 4.0 \times 10^{-5} \text{ inch } P/\text{lb} = 0.034 \text{ inch}$

$A_c = 4.0 \times 10^{-5} \text{ inch } C/\text{lb} = 0.082 \text{ inch}$

$$\beta = 16.26 \text{ arcmin}$$

$$T = 0.158 \text{ inch}$$

For the 140-ft geometry, we further have:

$$F = \text{focal length} = 720 \text{ inch}$$

$$b = \text{beam deviation factor} = 0.845$$

$$m = \text{magnification factor} \approx D/d - 1 = 13$$

### 3. Prime Focus Mode

The displacement of the apex (feed) from the best-fit focus is (up)

$$\Delta = W - A = (V - \alpha F) - (A_o + A_p) = 0.267 \text{ inch} \quad (31)$$

and the beam offset is (up)

$$\phi = \alpha - b \Delta/F \quad (32)$$

or

$$\phi = \alpha(1 + b) - \frac{b}{F}(V - A_o - A_p) \quad (33)$$

and numerically

$$\phi = 4.59 \text{ arcmin.} \quad (34)$$

From the angular terms of Table 1, we have, from zenith to horizon along the meridian,

$$\Delta D = P_4 \{ \sin(-51.6) - \tan 38.4 \cos(-51.6) \} = -1.276 P_4 \quad (35)$$

With the sign definition of equation (20) we should have  $\Delta D = -\phi$ , and from the calculated offset (34) we should expect  $P_4 = 4.59/1.276 = 3.60 \text{ arcmin}$ , whereas the observed values of Table 1 give only  $P_4 = 0.63 \dots 0.94 \text{ arcmin}$ . This is the disagreement discussed above.

Another question occasionally raised is whether or not a difference  $\delta P$  in box weight could cause a pointing error. According to the analysis, the error  $\delta\phi$  is

$$\delta\phi = \frac{b}{F} 4.0 \times 10^{-5} \delta P. \quad (36)$$

Receiver box weights may cover the range  $P = 600 \dots 1100$  lb, or  $\delta P = \pm 250$  lb, which gives the (negligible) error

$$\delta\phi = \pm 2.4 \text{ arcsec, max.} \quad (37)$$

#### 4. Cassegrain Mode

The displacement of the Cassegrain mirror from the best-fit paraboloid axis is (down)

$$\Delta_c = - (V - \alpha F) + (A_o + A_c) + \frac{F}{m+1} \beta = 0.024 \text{ inch} \quad (38)$$

and the feed displacement from the best-fit vertex is (up)

$$\Gamma = V - T = 1.602 \text{ inch.} \quad (39)$$

The resulting beam offset then is (A. M. Isber; Microwaves, Aug. 1967, p. 40)

$$\phi = \begin{array}{cccc} \alpha & - & \frac{2b}{m} \beta & + \frac{b}{F} \frac{m-1}{m} \Delta_c & - & \frac{b}{mF} \Gamma \\ \text{prim. rot.} & & \text{Cas.rot.} & \text{Cas.displ.} & & \text{feed displ.} \end{array} \quad (40)$$

or

$$\phi = \alpha \left(1 + \frac{m-1}{m} b\right) - \frac{b}{F} \left\{ V - \frac{m-1}{m} (A_o + A_c) - \frac{1}{m} T \right\} - \frac{b}{m} \frac{m+3}{m+1} \beta \quad (41)$$

and numerically

$$\phi = 3.15 \text{ arcmin.} \quad (42)$$

For comparison, we have entered in Table 1 also the pointing parameters for Cassegrain mode, as obtained by K. Kellermann on Jan. 13, 1975, with

$\lambda = 6$  cm wavelength. Again, the observed value  $P_4 = 0.86$  arcmin does not agree with the calculated value  $\phi/1.276 = 2.47$  arcmin.

Only  $P_4$  and  $P_9$  should be different for Cassegrain and prime focus modes. All other parameters should be the same for both modes. Table 1 gives indeed fairly good agreement, except for  $P_{10}$  and  $P_{11}$  which may be explained by their error correlation with  $P_9$ . Large deviations occur also for the two non-physical parameters,  $A_{10}$  and  $A_{12}$ .

The Cassegrain mirror is balanced by a counterweight such that it does not give a rotational moment about the apex. But when the focal adjustment is changed by  $\delta F$ , this gives a moment  $M = (\frac{1}{3} S + C) \delta F$  assuming that about 1/3 of the sterling weight is moved. The analysis yields an apex rotation of  $\delta\beta = 4.47 \times 10^{-5}$  arcmin M/inch lb. According to Electronics Div. Int. Report 160 of May 1975, the automatic gravitational focal adjustment is 17.6 mm between zenith and horizon, and in addition there may be a thermal focus change of 2.07 mm  $\Delta T/^\circ\text{C}$ . The largest measured temperature difference between declination wheel and shaft, Table 5, is  $\Delta T = 3.8$   $^\circ\text{C}$ , giving a thermal focus change of  $2.07 \times 3.8 = 7.9$  mm. In total, the maximum focus change then is  $\delta F = 25.5$  mm or 1.0 inch, and the maximum apex rotation is  $\delta\beta = 0.110$  arcmin = 6.6 arcsec, which also causes a small displacement of the mirror. The resulting beam offset  $\delta\phi$ , from both rotation and displacement, is fortunately negligible:

$$\delta\phi = \frac{b}{m} \frac{m+3}{m+1} \delta\beta = 0.49 \text{ arcsec max.} \quad (43)$$

It is a pleasure to thank Tom Cram, Claude Williams, Ken Kellermann, and especially Fred Crews for the considerable amount of help I got from each of them.

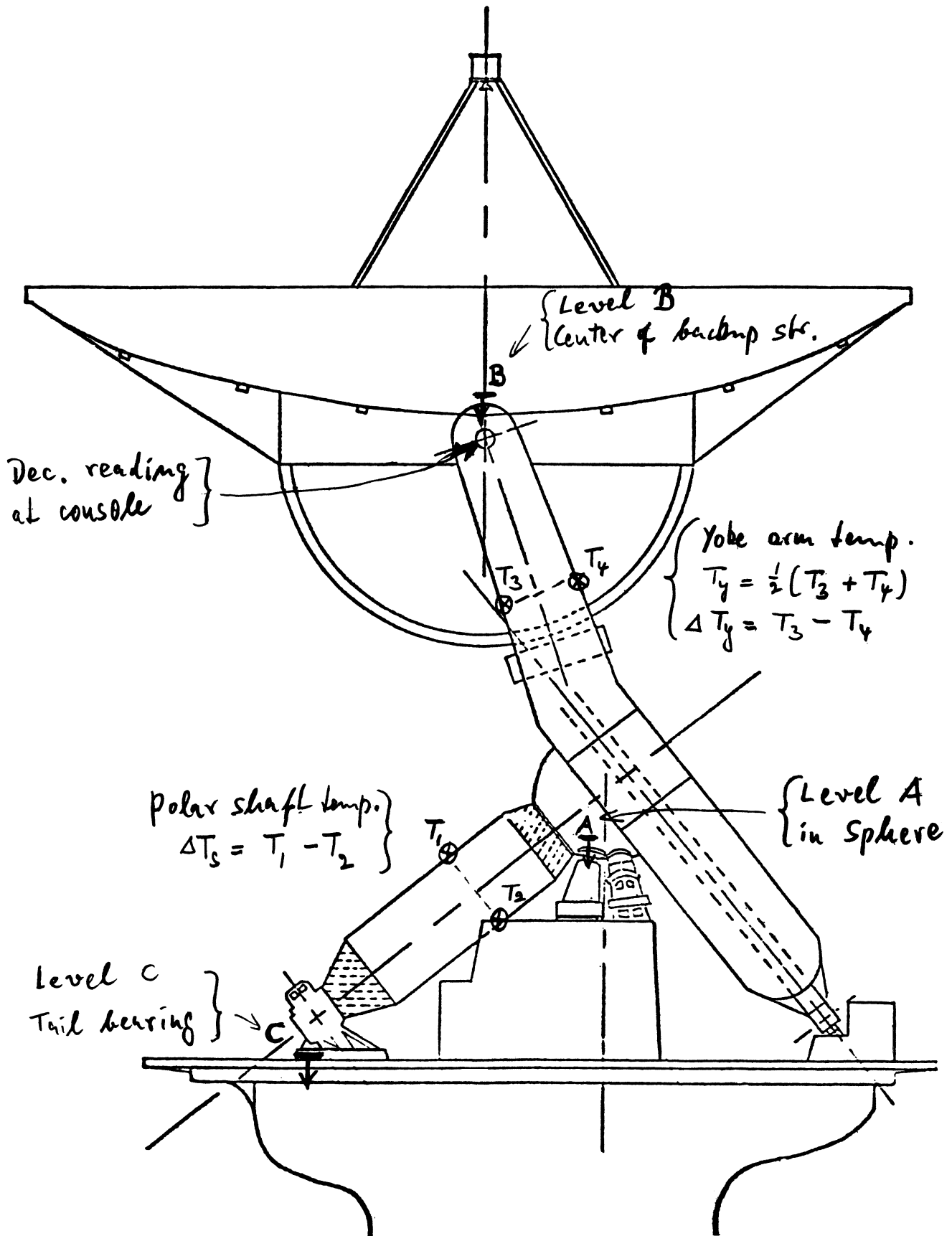


Fig. 1. Locations of four thermistors and three electronic levels.  
 For all levels, "+" is South. For the Declination reading  
 at the console, "+" is North. Declination error = B + Dec.

-10 -10 0 2 4 6 8 10 2 4 6 8 20 2 4 6 8

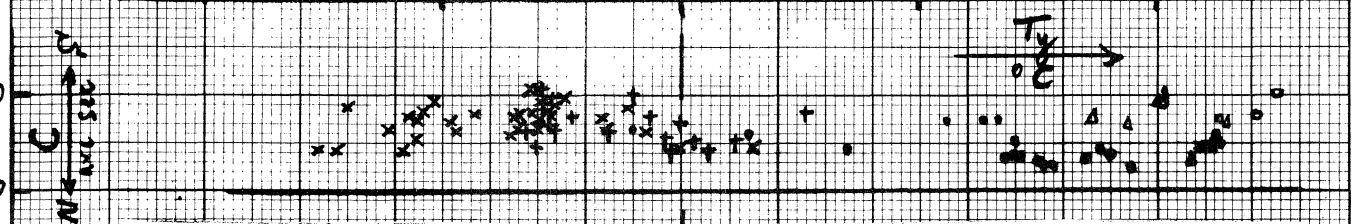


Fig. 2. Level C at tailbearing, versus yoke temperature  $T_y$  which serves as a measure for the smoothed air temperature.

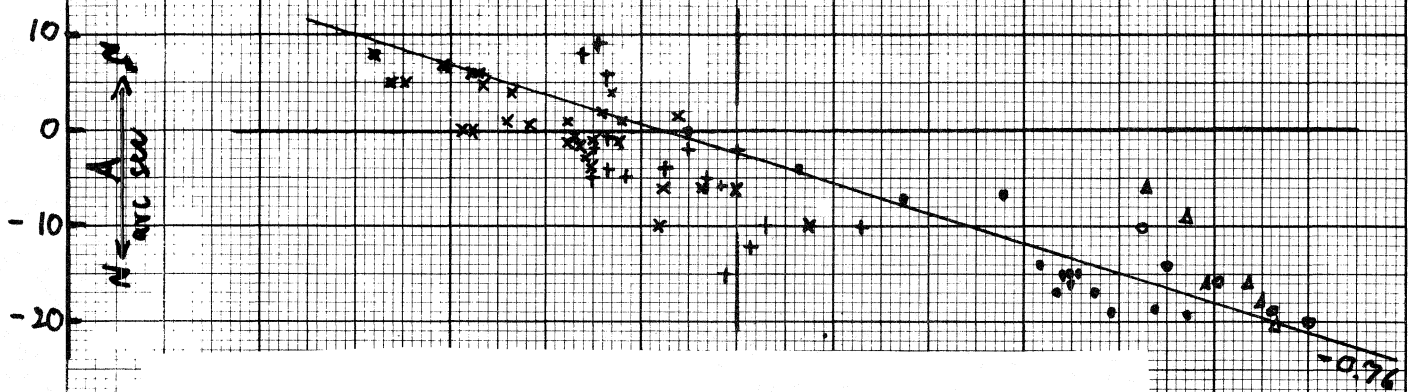


Fig. 3a. Level A in sphere, versus  $T_y$ . For symbols see text.

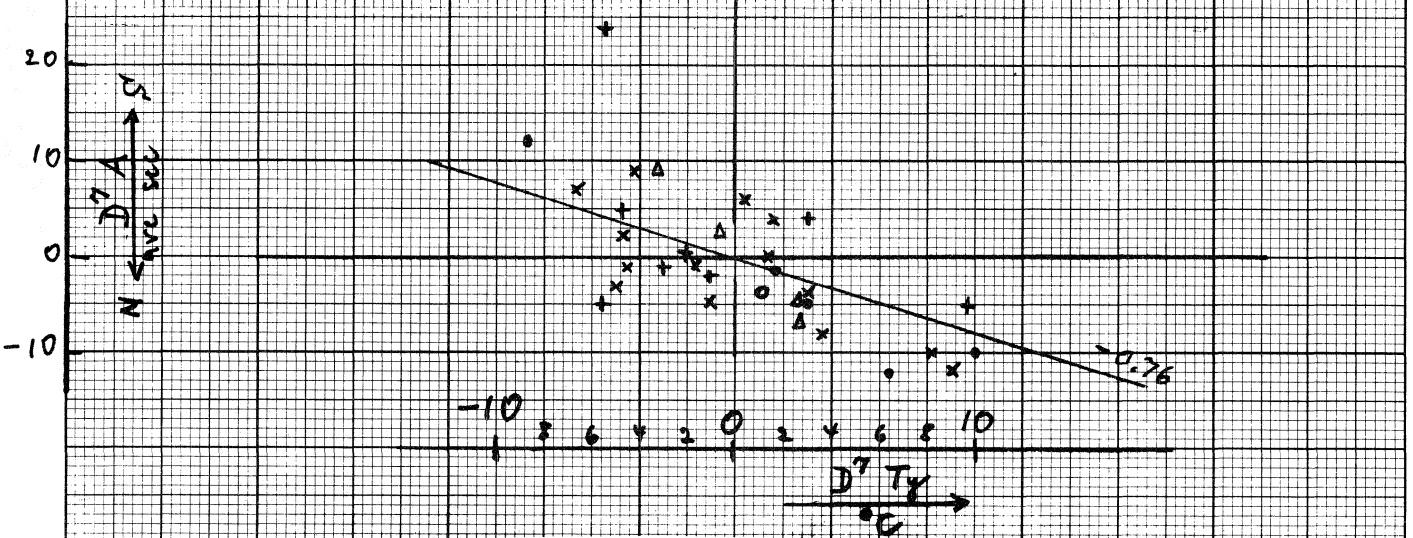


Fig. 3b. Changes of A and  $T_y$ , during 7 days.

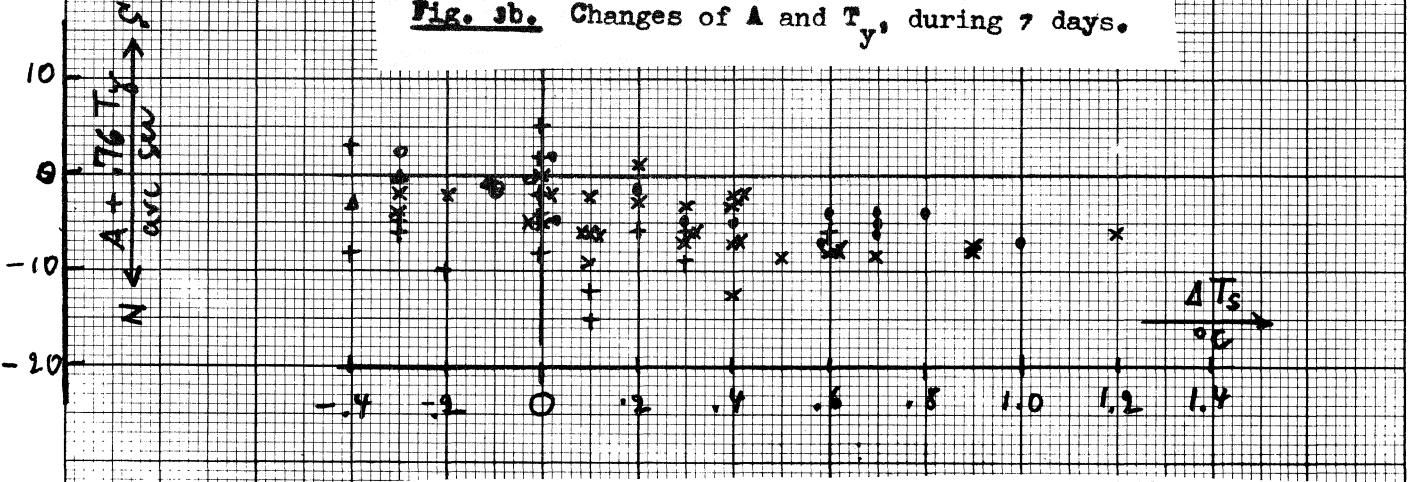
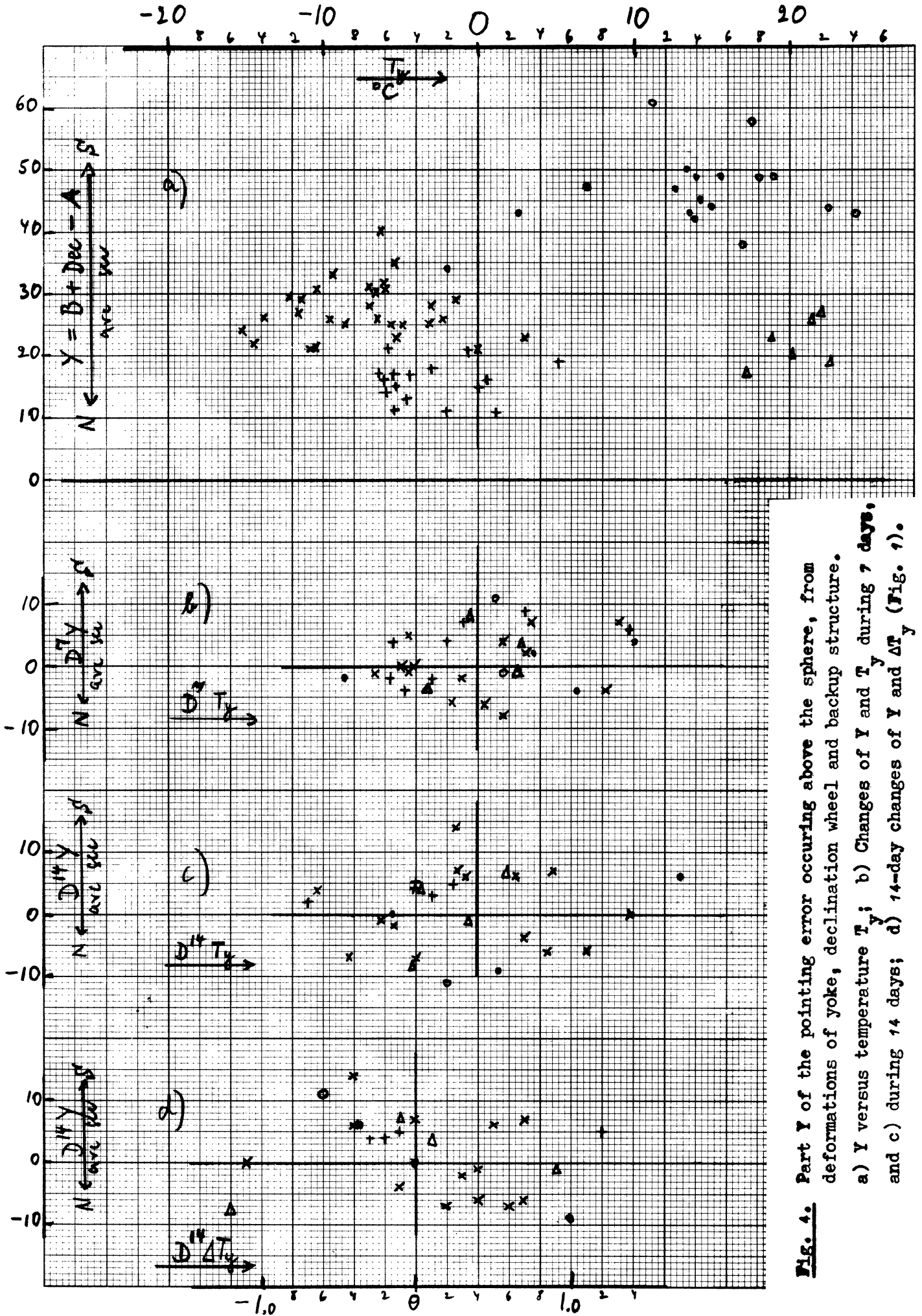
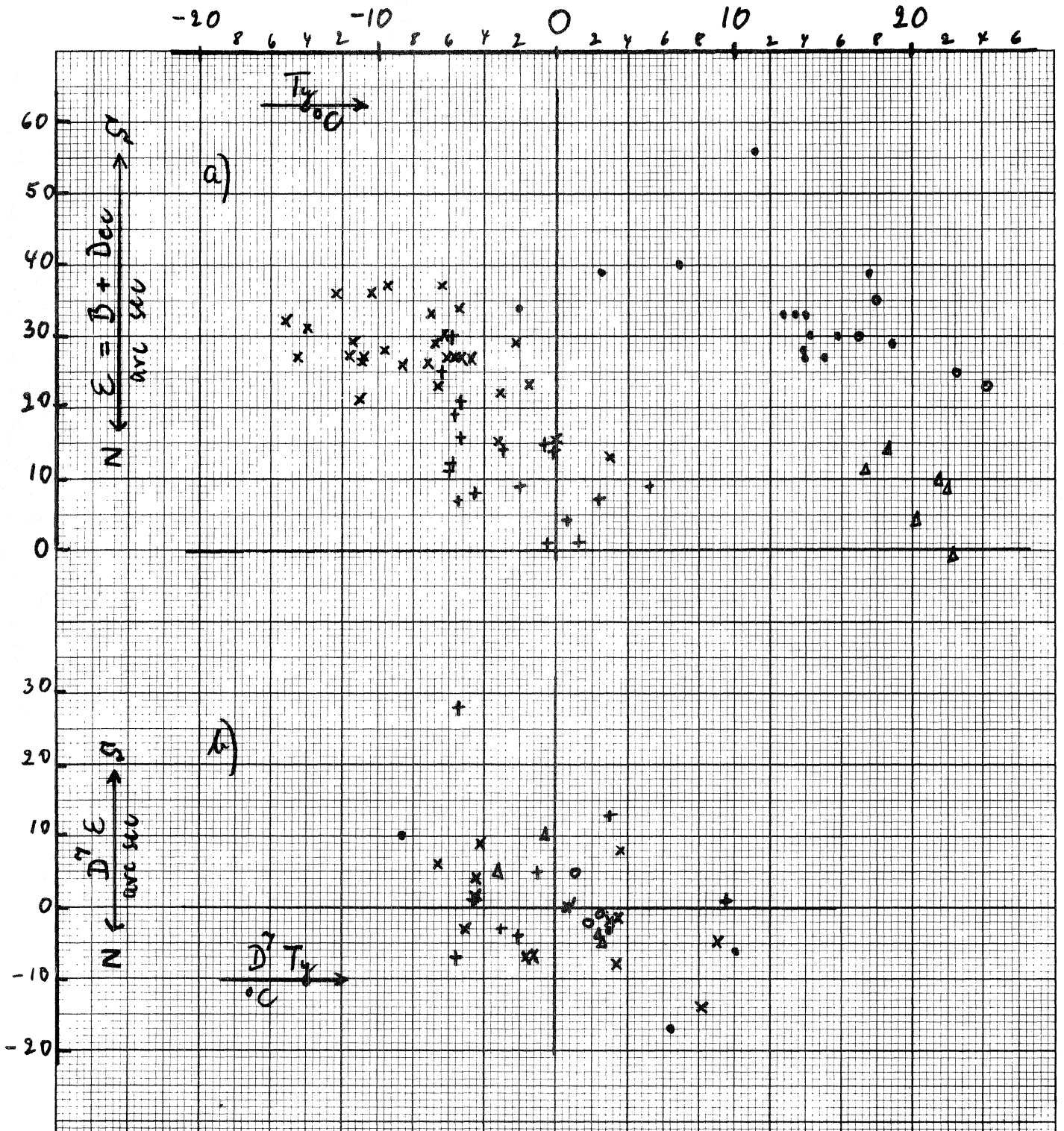


Fig. 3c. Residuals from Fig. 3a, versus temperature difference across polar shaft (see Fig. 1).





**Fig. 4.** Part Y of the pointing error occurring above the sphere, from deformations of yoke, declination wheel and backup structure.  
a) Y versus temperature  $T_y$ ; b) Changes of Y and  $T_y$  during 7 days, and c) during 14 days; d) 14-day changes of Y and  $\Delta T_y$  (Fig. 1).



**Fig. 5.** Declination pointing error  $E$ .

- a) Versus temperature  $T_y$ ;
- b) Changes during 7 days.

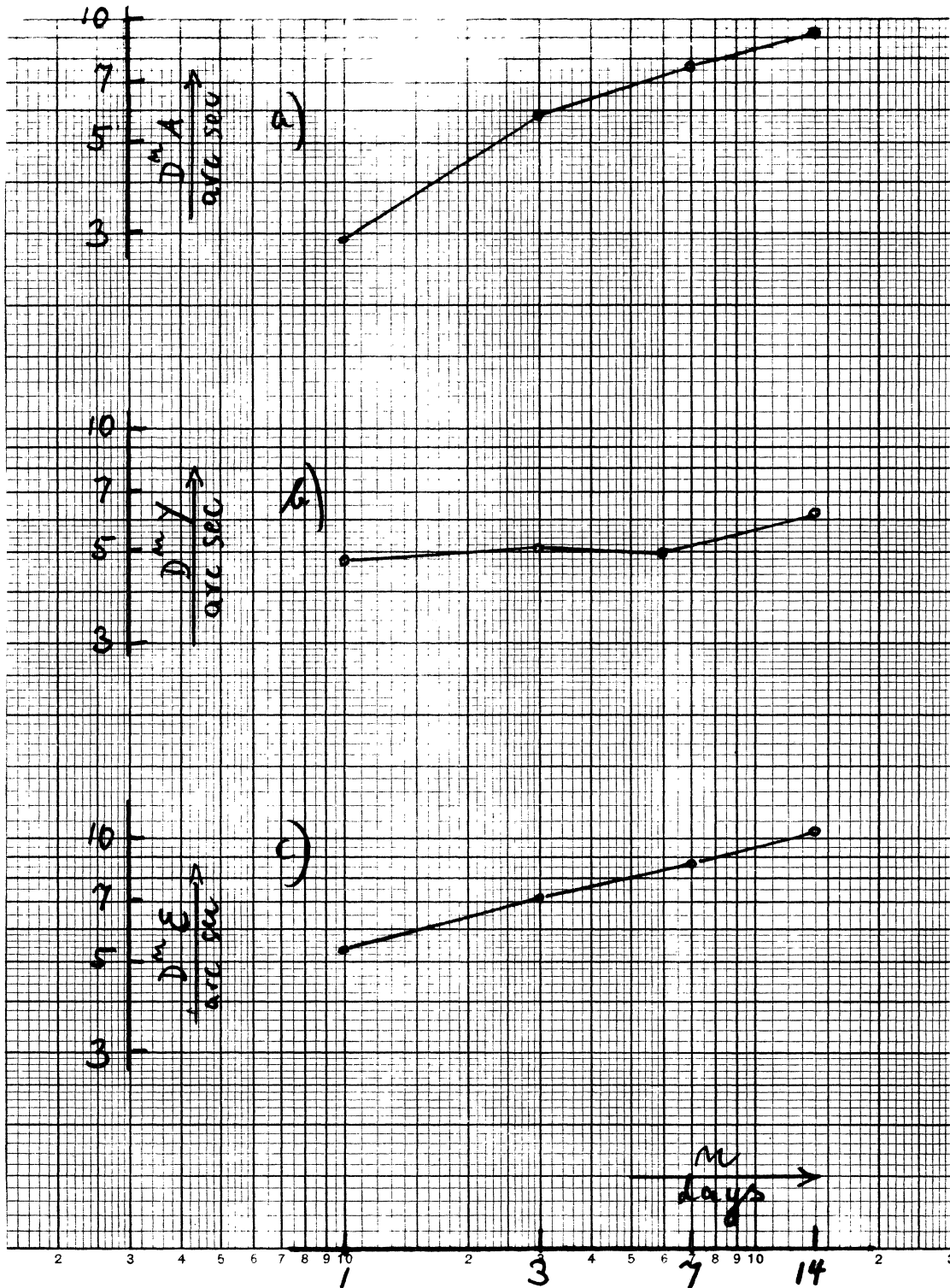


**Fig. 6.** Rms changes during n days, of readings taken at 8:00 EST.

- a) Concrete building and shaft;
- b) Deformations above the sphere;
- c) Declination pointing error.

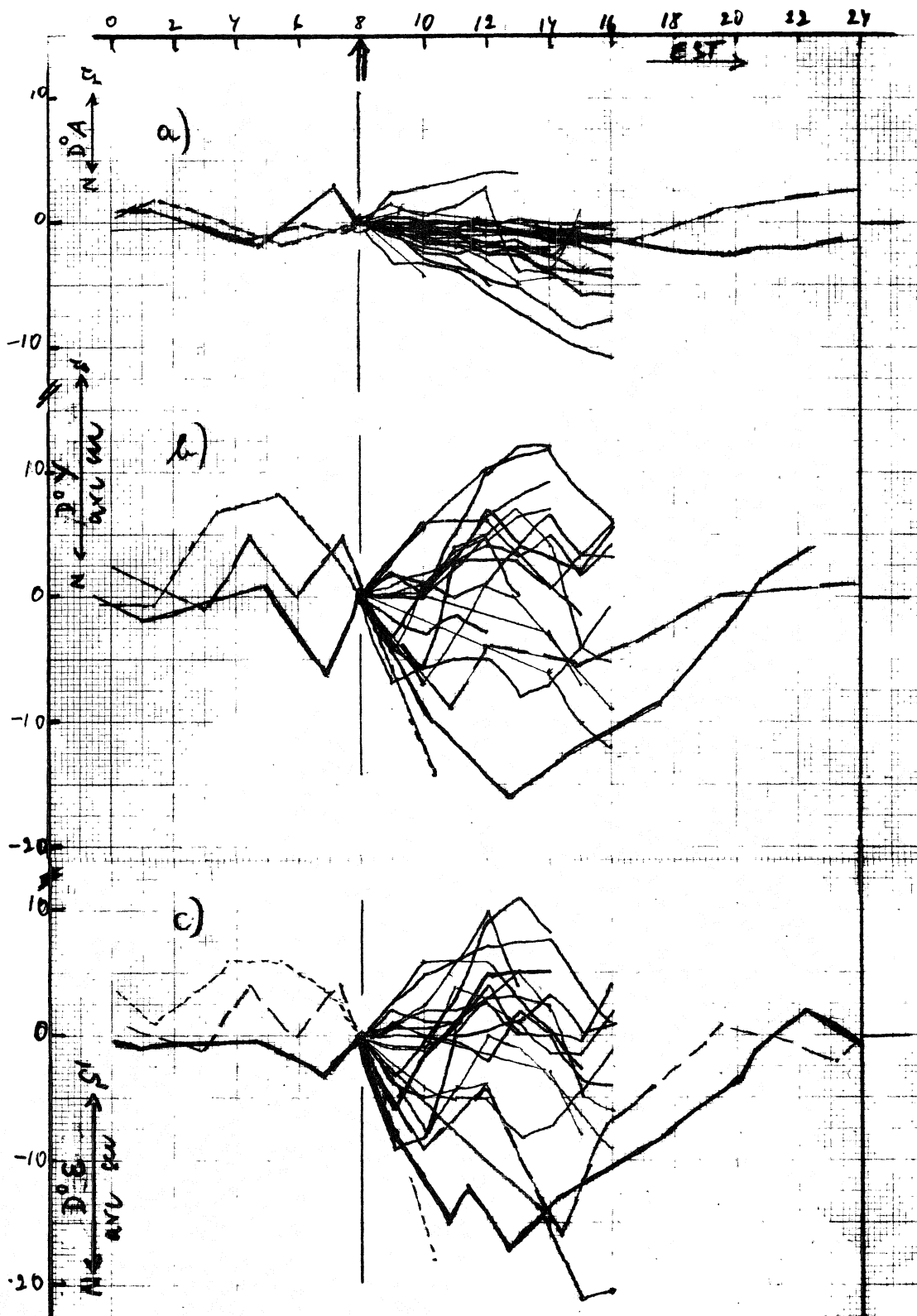
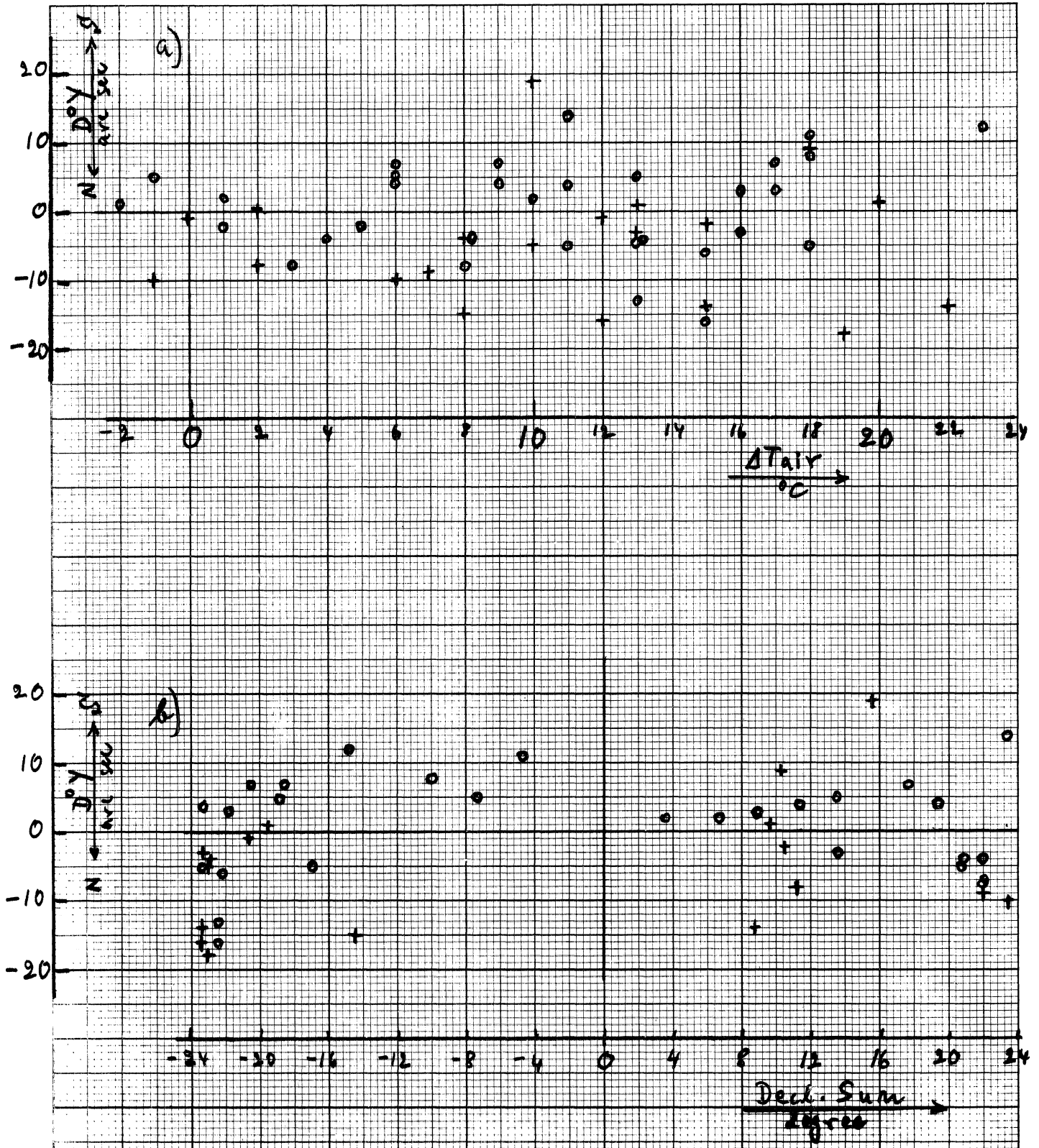


Fig. 7. Thermal deformations during sunny days (normalized at 8:00 am).

- a) Concrete building and shaft;
- b) Deformations above the sphere;
- c) Declination pointing error.



**Fig. 8.** Deformations  $D^0Y$  above sphere, between 8 and 14 EST of same day.  
 + telescope was moved in between; o not moved.

- a) As function of sunshine, measured in terms of  $\Delta T^{\text{air}}$  = increase of ambient air temperature;  
 b) As function of the Sun's declination (for  $\Delta T^{\text{air}} \geq 6^{\circ}\text{C}$  only).



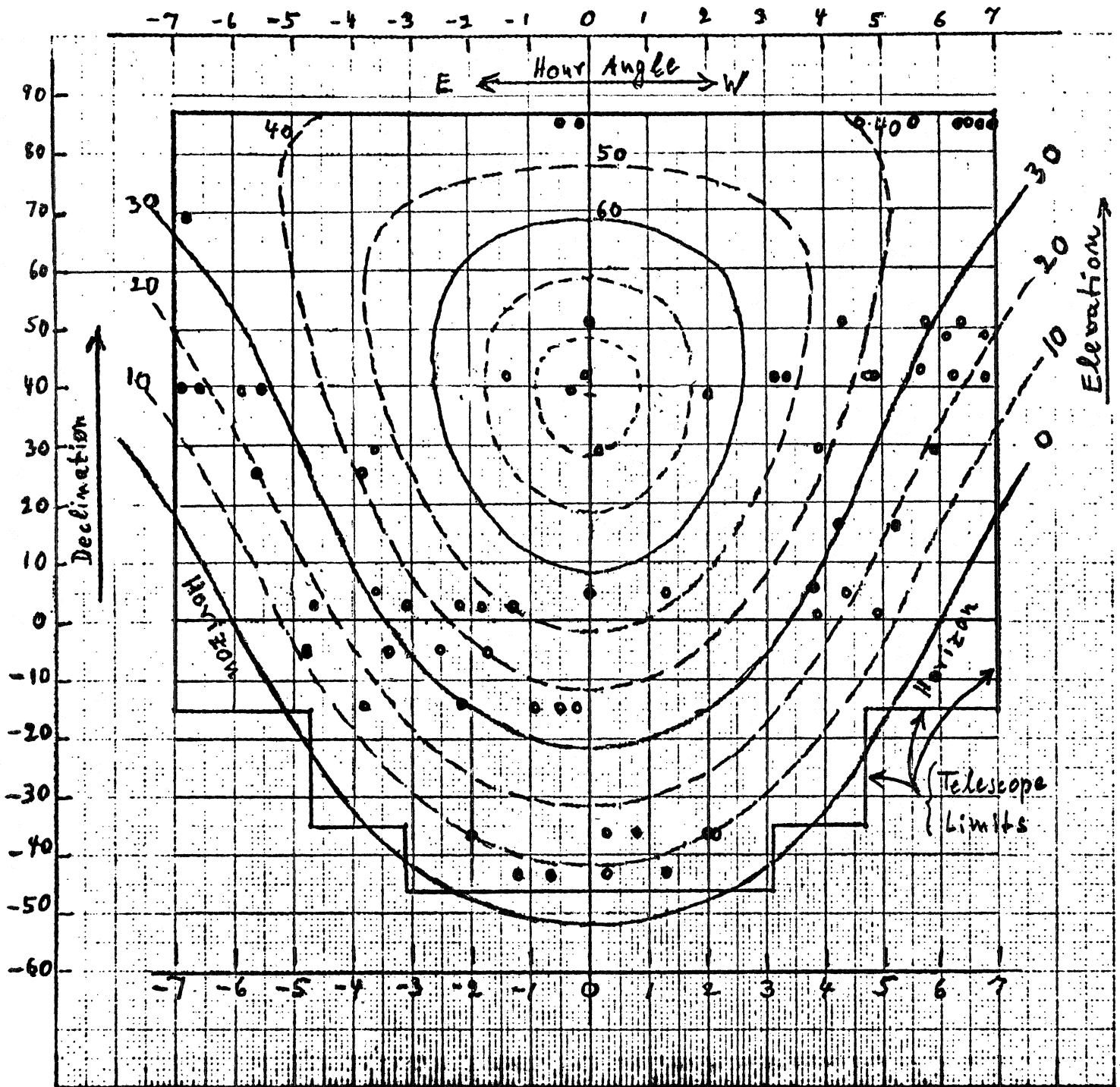
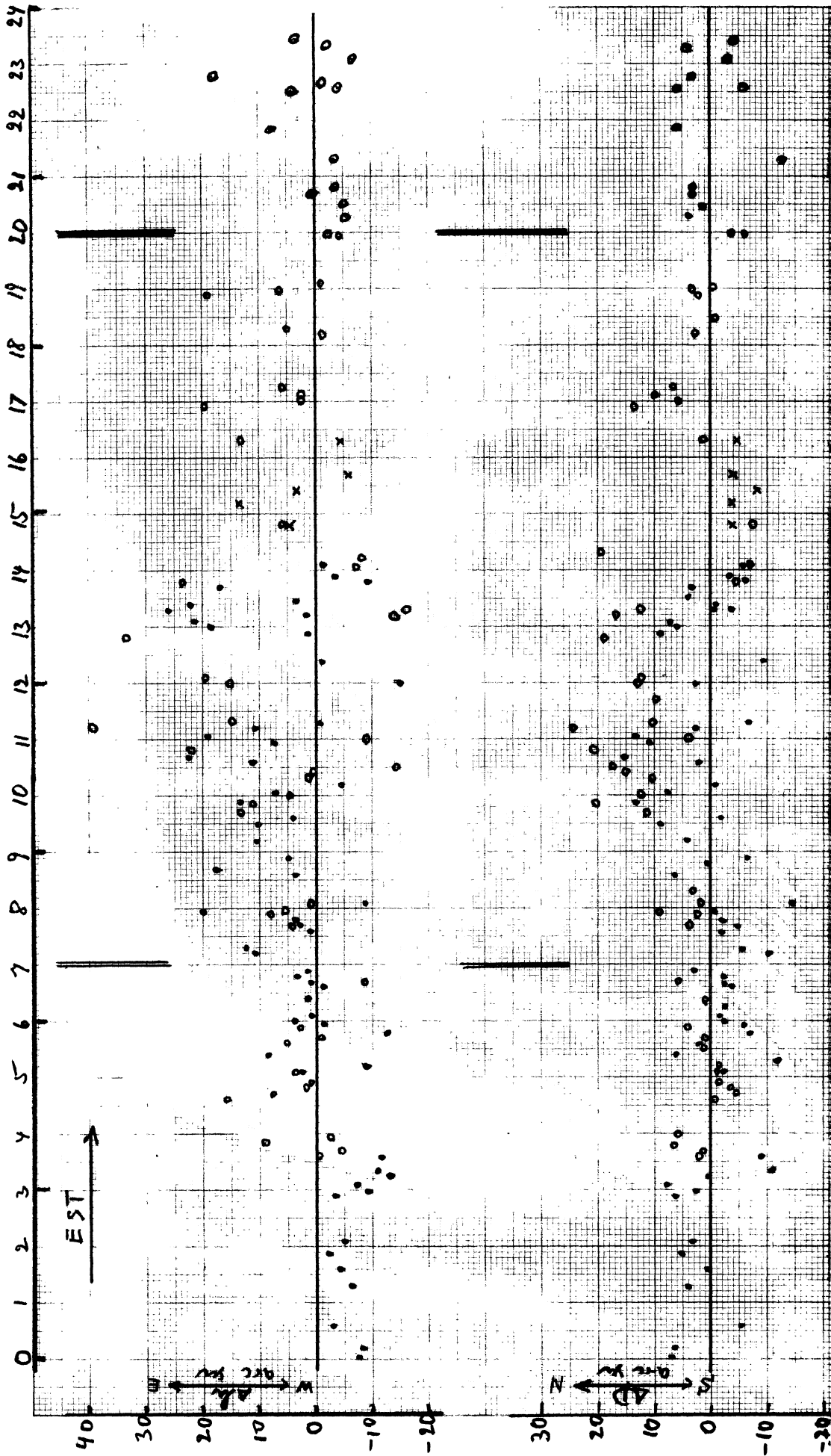


Fig. 9. Sky distribution of the 68 present night observations, for determination of the new 11 pointing parameters.



**Fig. 10.** Observed pointing errors during 24 hours, on three sunny days and two nights.

Residuals from 11 new parameters of "night" solution.

The signs (NS, EW) mean actual physical movement of structure and building.

Three weak sources are omitted.

✕ Dec. 2; ● Dec. 3; ○ Dec. 4.

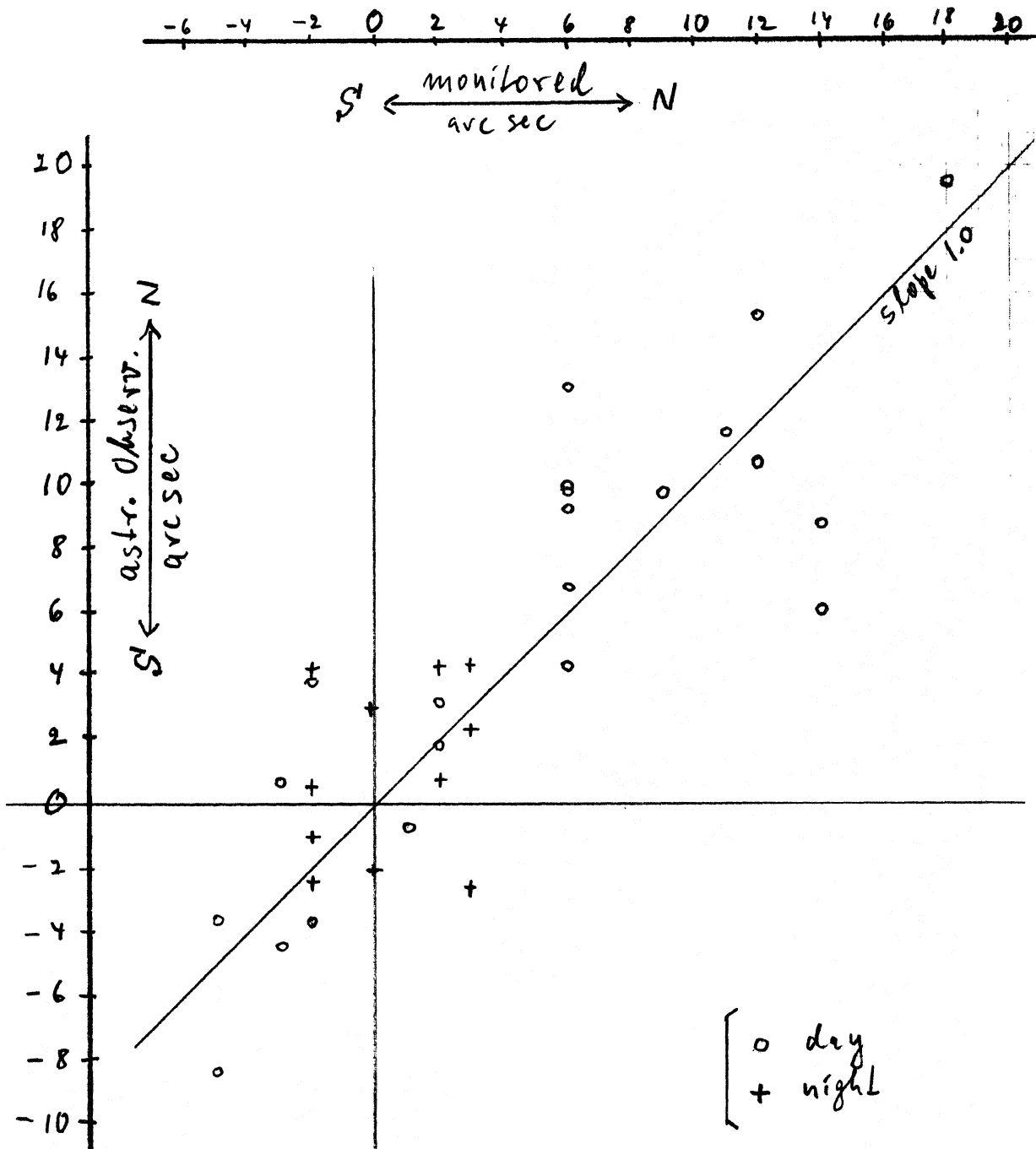


**Fig. 19.** Correlation between the declination pointing error observed astronomically with radio sources, and the error monitored at the electronic level B in zenith position, for all cases where the time difference between the two was less than 25 minutes. Two weak sources are omitted.



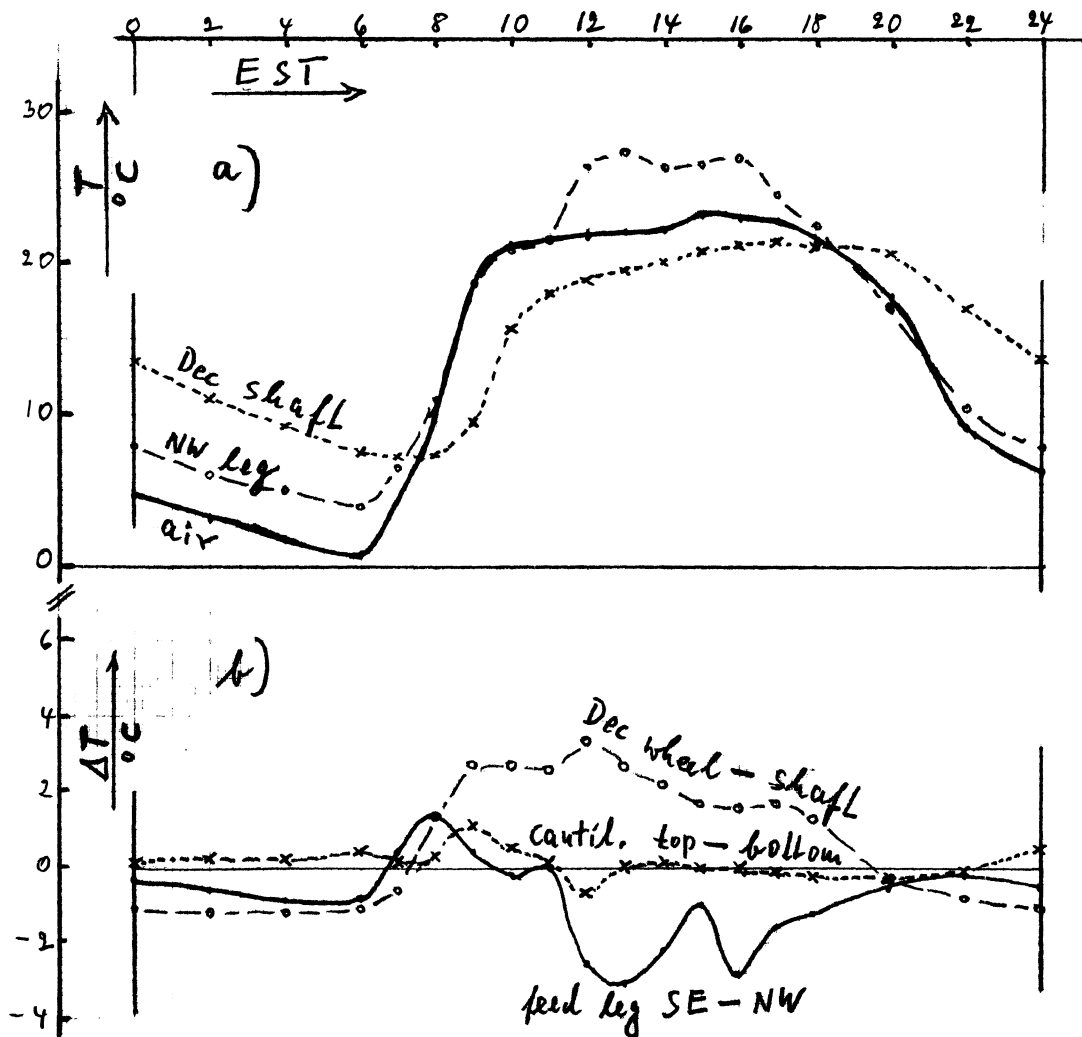


**Fig. 12.** Temperature measurements in the upper structure. Shown is the day with the largest temperature differences  $\Delta T$  (out of 270 recorded days), April 12, 1977, with an air raise of  $\Delta T_{\text{air}} = 22.7^{\circ}\text{C}$ .

- a) Temperatures of declination shaft, NW feed leg, and ambient air.
- b) Temperature differences  $\Delta T$ .

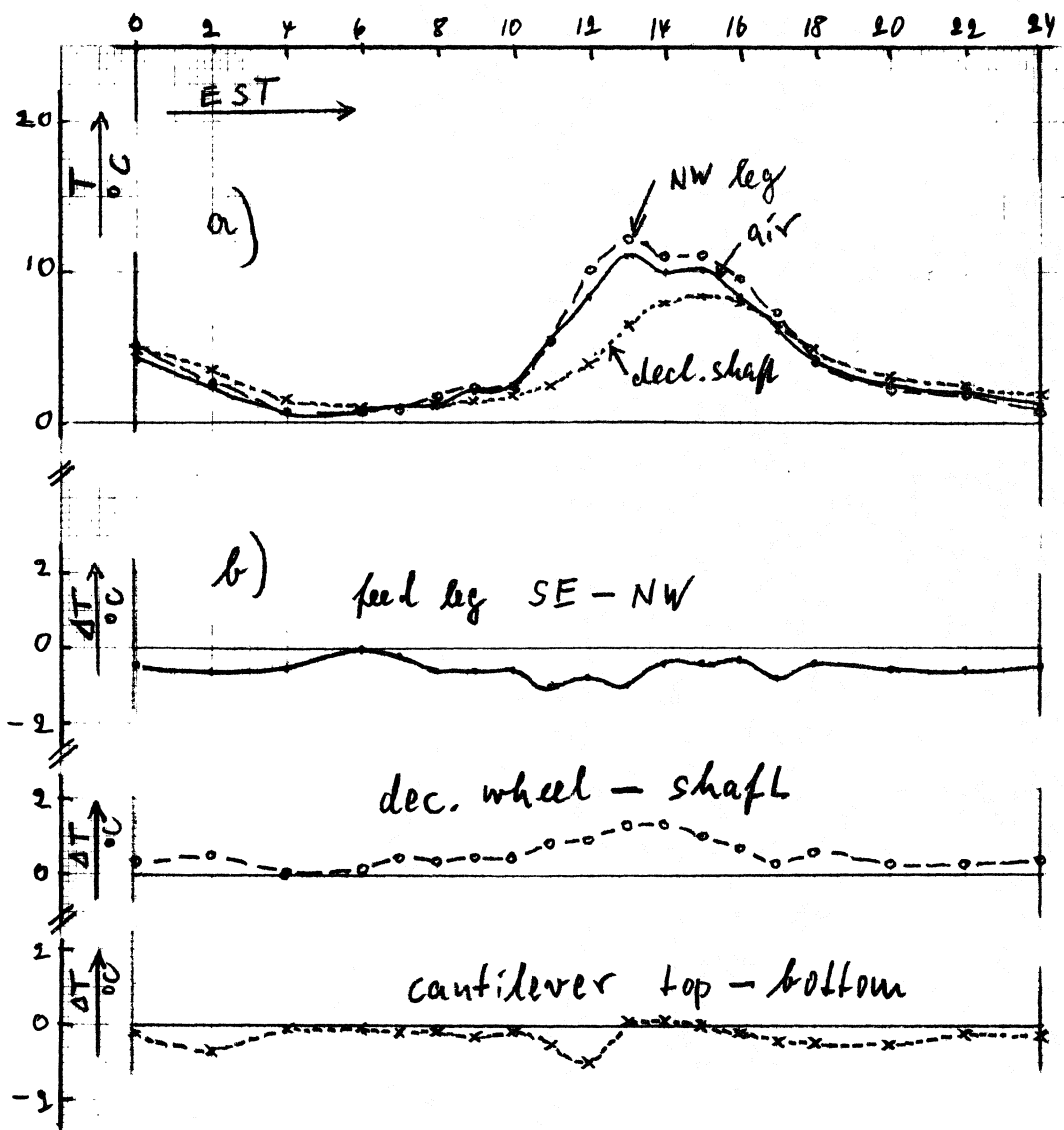


**Fig. 13.** Same as Fig. 12, but for an average day, March 20, with  $\Delta T_{\text{air}} = 10.5^{\circ}\text{C}$ .

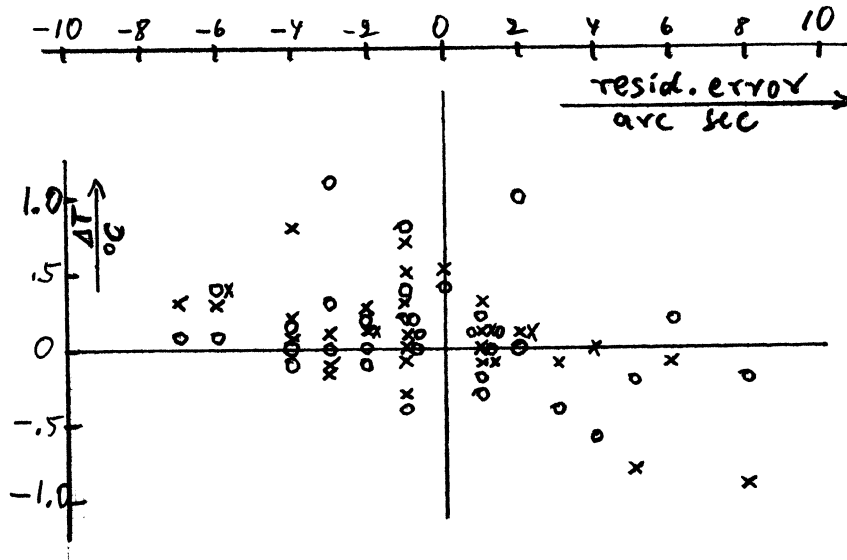
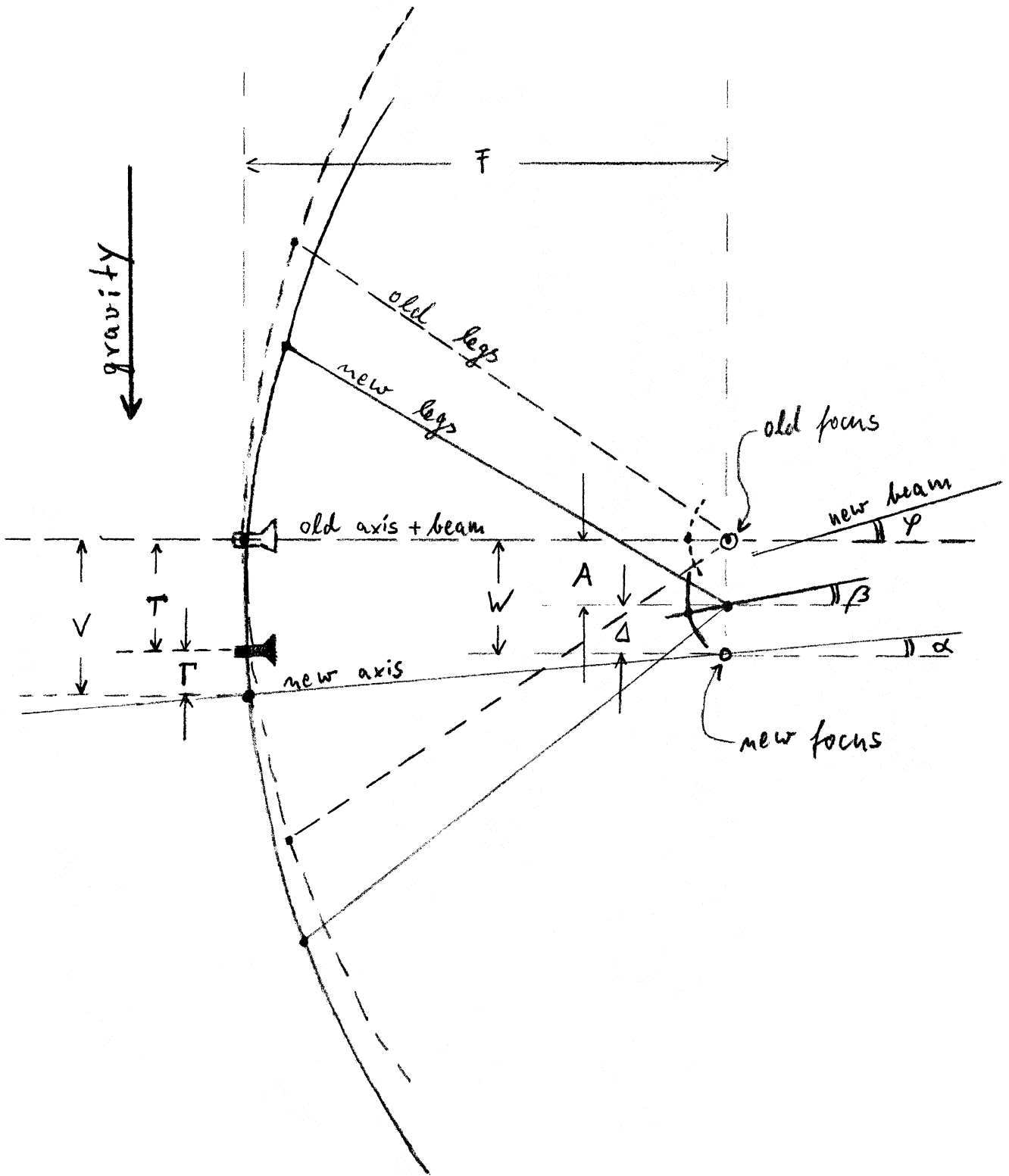


Fig. 14. Residual pointing errors from Fig. 11 (electronic level B minus astronomical observation), and temperature differences  $\Delta T$  in the upper structure.

$\Delta T$  { o feed legs, SE - NW;  
 x NE cantilever, top - bottom.



**Fig. 15.** Geometry of gravitational deformations.

- old, undeformed
- new, deformed